



# Electrodeposition Technique to Fabrication CIGS using Pure Selenium and $\text{SeO}_2$ as Selenium Source

Hilda Rahmawati<sup>a</sup>, M Tommy Hasan Abadi<sup>a</sup>, Siti Zulaikah<sup>a</sup>, Nandang Mufti<sup>a,b,\*</sup>

<sup>a</sup> Department of Physics, Faculty of Mathematics and Natural Sciences, Universitas Negeri Malang, Jl. Semarang 5 Malang 65145, Indonesia; <sup>b</sup> Centre of Advanced Materials for Renewable Energy (CAMRY), Universitas Negeri Malang, Jl. Semarang 5 Malang 65145, Indonesia.

**Abstract** Energy demands are increasing day by day because almost all equipment that supports human activities uses electrical energy. CIGS solar cells are an energy source that is environmentally friendly, renewable, and has high efficiency. Selenium is one of the materials used in making solar cell CIGS. However, researchers often find the problems of this material hard to dissolve compared to other materials (copper, indium, and gallium). Therefore, in this study, pure selenium will be synthesized to produce selenium dioxide ( $\text{SeO}_2$ ) as a material for making solar cell CIGS with electrodeposition. The XRF showed the resulting selenium dioxide of 99.077%, SEM-EDX showed At% selenium from  $\text{SeO}_2$  greater than pure selenium, XRD showed CIGS orientation on (211) and (105).

**Keywords:** Energy, Selenium, Selenium dioxide, CIGS, Electrodeposition.

## Introduction

CIGS (Copper, Indium, Gallium, Selenium) are solar cells formed from the combined inorganic type-P compounds, which are included in the I-III-VI group in the periodic table [1][2][3]. CIGS have compatibility used as solar cells because of high light absorption, can last a long time, and feasibility for large scale [4]. In addition, the CIGS has a range of gap bands around 1.01 eV to 1.60 eV, which easy electron transfers when under sunlight, and the value of density and electron mobility is  $10^{12} \text{ cm}^{-3}$  and  $10 \text{ cm}^2/\text{VS}$  [5].

Currently, various methods have been developed in the manufacture of CIGS films. Some of the methods offered require special equipment, for example co-evaporating [6], sputtering [7], and heating-up [8]. Which produces a uniform microstructure and good electrical properties, but this technique requires vacuum conditions and always maintains air pressure conditions under certain conditions. Otherwise, non-vacuum methods can be performed at room temperatures, such as electrodeposition [9], spin coating [1], and spray pyrolysis [10]. Among these techniques, electrodeposition is the most preferred method because it is simple, does not require vacuum equipment, thus reducing the cost of production, is stable, and has also been proven to produce CIGS absorbing layers in previous studies [4].

In general, the selenium coating of CIGS is derived from pure selenium obtained commercially. However, this has a weakness when scale-up production is carried out due to cost constraints. In addition, in the

**\*For correspondence:**  
nandang.mufti.fmipa@um.ac.  
id

**Received:** 1 Nov 2021  
**Accepted:** 6 March 2022

© Copyright Rahmawati *et al.* This article is distributed under the terms of the [Creative Commons Attribution License](#), which permits unrestricted use and redistribution provided that the original author and source are credited.

CIGS fabrication process, selenium requires special conditions under a nitrogen atmosphere and requires a special solvent to dissolve [3]. Therefore, a material solution is needed to overcome this problem, using selenium dioxide ( $\text{SeO}_2$ ) as a selenium source. Selenium dioxide ( $\text{SeO}_2$ ) has various uses, including cheap and easy to obtain, thereby reducing production costs, has high chemical stability [11], does not require special solvents, and can be used as a material for CIGS solar cells [12].

Therefore, this study will fabricate a  $\text{SeO}_2$ -based CIGS layer as a substitute for pure selenium using the electrodeposition method. Meanwhile, a pure selenium-based CIGS layer will be used as a control variable.

## Materials and methods

### *Synthesis of $\text{SeO}_2$*

5 grams of selenium powder was added to 2.5 ml of aquadest, then stirred for 120 minutes at 150 rpm at room temperature. After that, add 7.74 ml of hydrogen peroxide ( $\text{H}_2\text{O}_2$ ) to the solution, stir for 120 minutes at 150 rpm. After the solution is formed, let stand for 24 hours at room temperature. Next, filter the solution using filter paper. Finally, the filtered powder was dried using a hotplate for 60 minutes at  $100^\circ\text{C}$ . This procedure is shown in Figure 1.

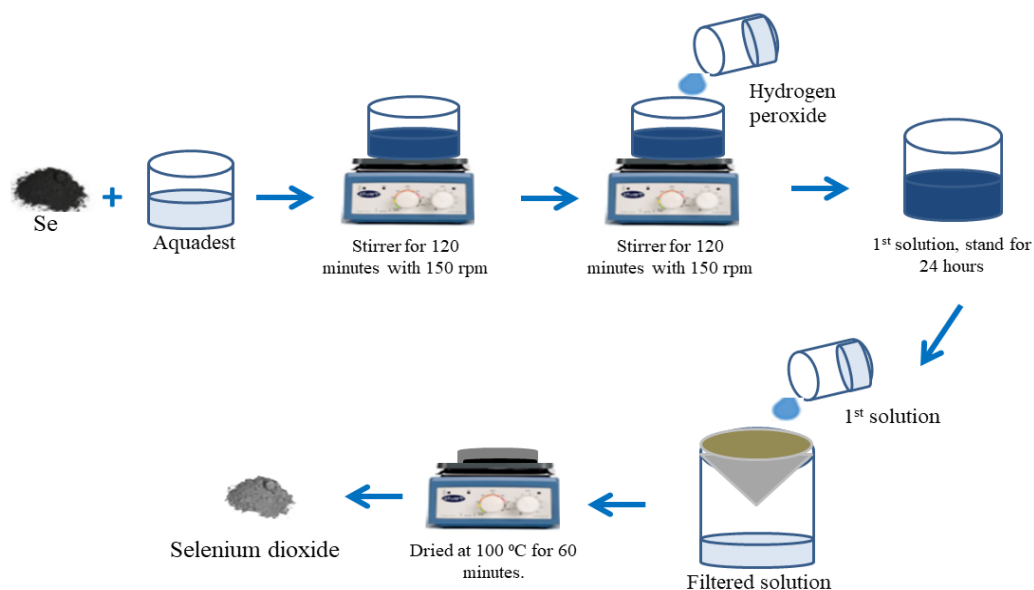


**Figure 1.** Synthesis selenium dioxide

### *CIGS deposition with electrodeposition*

The CIGS absorber layer film in this study was carried out using the two-electrode electrodeposition method. The precursor used in this study was 3 Mm  $\text{Cu}(\text{acac})_2$ , 3 Mm  $\text{InCl}_3$ , 0.9 Mm  $\text{Ga}(\text{acac})_2$ , 8 Mm Se (with pure Se and  $\text{SeO}_2$ ), which was dissolved in DI water, then dripped with HCl to adjust the pH solution of 1.7. In the electrodeposition process, a voltage of -1.5 V was applied. The resulting thin film was then annealed at  $350^\circ\text{C}$  for 30 minutes. After that, fabrication ITO/CIGS/ZnS with chemical bath deposition (CBD) and ITO/CIGS/ZnS/ZnO with spin coating method.

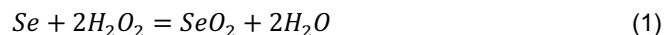
## Results and discussion

X-Ray Fluorescence (XRF) is a tool that can analyze the composition contained in a sample/material by utilizing the interaction between x-rays and materials [13]–[15]. The synthesized selenium was then tested using XRF to determine the elemental composition contained in the sample. Table 1 shows the results of the XRF analysis of the synthesized selenium samples.

**Table 1.** Chemical compounds sample selenium determined by XRF spectroscopy.

| Chemical Compound              | Composition (%) |
|--------------------------------|-----------------|
| P <sub>2</sub> O <sub>5</sub>  | 0.47            |
| CaO                            | 0.16            |
| Cr <sub>2</sub> O <sub>3</sub> | 0.035           |
| Fe <sub>2</sub> O <sub>3</sub> | 0.078           |
| NiO                            | 0.059           |
| CuO                            | 0.041           |
| SeO <sub>2</sub>               | 99.077          |
| PtO <sub>2</sub>               | 0.08            |

Based on the XRF results in Table 1, the total elemental composition is 100%, with selenium dioxide produced at 99.077%. This shows that pure selenium has been successfully synthesized into selenium dioxide. Selenium dioxide (SeO<sub>2</sub>) can be formed due to the reaction between selenium and hydrogen peroxide so that there will be oxidation of elements by peroxide [16], [17]. According to the following reaction:



Slowly adding hydrogen peroxide to a concentrated aqueous solution of pure selenium, which is not exceeded stoichiometrically by reaction (1), yields selenium dioxide [18]. Based on the data from Table 1, it was found that the selenium produced had a high purity, reaching 99.077%. This indicates that the research conducted did not exceed the stoichiometry of the reaction (1). Therefore, it will affect the peak in the XRD results with a high purity level, and the CIGS peak will be more dominant if using selenium dioxide as a source of selenium.

Figure 2 shows the diffraction pattern of CIGS with selenium source from pure selenium and selenium dioxide synthesized and deposited by electrodeposition method. Based on the High Score Plus analysis results, the sample diffraction pattern was obtained, which corresponds to the reference code 01-073-1667, and the diffraction peak of the sample also corresponds to previous studies [19][3]. In the study of Mankoshi *et al.* [19], several CIGS peaks were found at  $2\theta=26.91^\circ$ ,  $28.02^\circ$ ,  $35.48^\circ$ ,  $42.43^\circ$  until  $71.69^\circ$ . The CIGS sample is pure Se (Figure 2a), the CIGS peak is at  $35.34^\circ$  with orientation (211), and the other peaks are ITO peaks. In the CIGS samples with selenium as the source of selenium dioxide (Figure 2b), the CIGS peaks were at  $35.34^\circ$  with orientation (211) and  $42.11^\circ$  with orientation (105). Therefore, the peak that appears in the sample indicates that same several previous studies.

Based on Figure 2, there is one CIGS peak when using pure selenium as a selenium source and increases to two CIGS peaks when using selenium dioxide as a selenium source. This shows that the crystallinity of the film rises when using selenium dioxide (SeO<sub>2</sub>). In the CIGS deposition process using the electrodeposition method, soluble material is needed [20][2] because, in this method, the solvent used is a simple solvent, namely DI water. The nature of selenium dioxide, which is more soluble than pure selenium, causes the crystallinity of the CIGS films to increase when using selenium dioxide (SeO<sub>2</sub>) as a source of selenium. The crystal grain size was measured using the Debye-Scherrer equation, which is shown in Table 2.

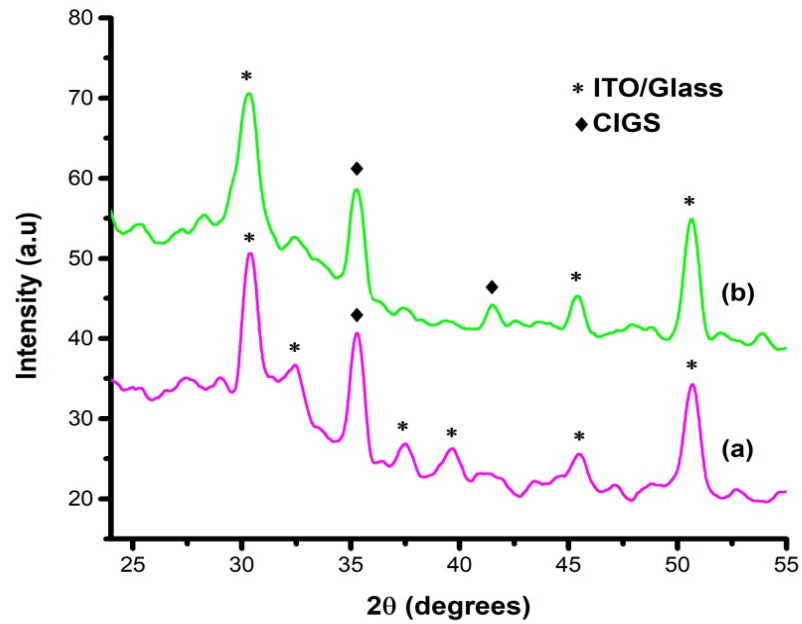


**Figure 2.** CIGS diffraction pattern with (a) Pure Se (b) SeO<sub>2</sub>

**Table 2.** Grain size of CIGS crystals with pure selenium (Se) and selenium dioxide (SeO<sub>2</sub>)

| No | Sample                     | FWHM   | Grain size (nm) |
|----|----------------------------|--------|-----------------|
| 1  | CIGS with Pure Se          | 0.2785 | 65.92           |
| 2  | CIGS with SeO <sub>2</sub> | 0.2671 | 57.72           |

Based on Table 2, the grain size of CIGS crystals with pure Se was 65.92 nm, and the grain size of crystals with SeO<sub>2</sub> was 57.72 nm. Thus, the grain size of CIGS crystals is reduced when using selenium as a source of selenium. This is following the research of Saidi *et al.*, where the crystal grain size of CIGS is at 53 nm – 82.50 nm [2].

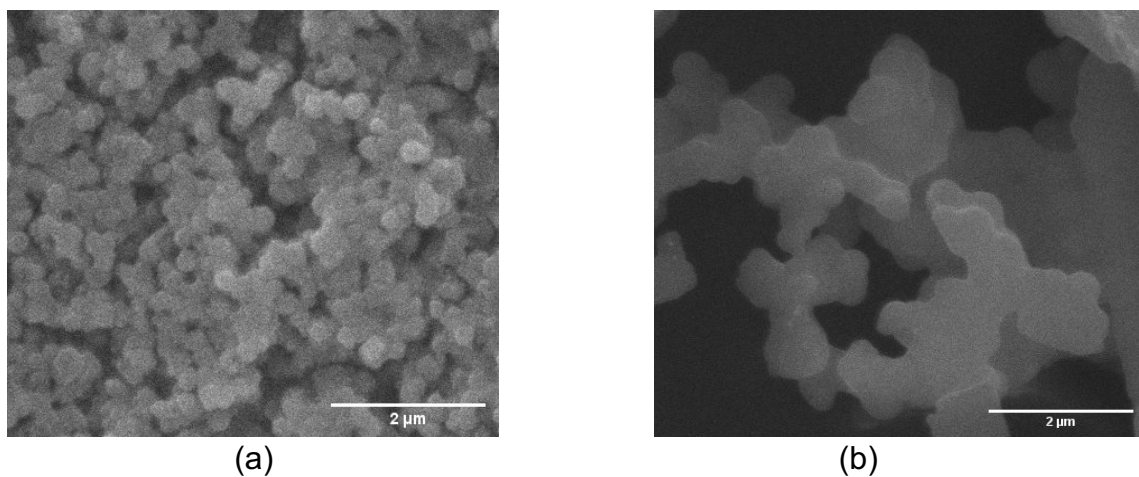


**Figure 3.** CIGS morphology with (a) Pure Se (b) SeO<sub>2</sub>

A scanning electron microscope (SEM) is a tool used to analyze the surface or morphology of samples with magnification using a particular scale. Figure 3 shows the morphological structure of CIGS by (a)

using pure selenium and (b) using selenium dioxide from SEM. Based on Figure 3, the morphology on the surface of the two samples tends to be round, rough, and irregular. This is following several previous studies [2], [21]. CIGS electrodeposition process using selenium dioxide as a source of selenium, the morphology was almost the same as Aigul *et al.* [22], where there is agglomeration on the sample surface. The average particle size distribution of CIGS films with pure Se and SeO<sub>2</sub> was 79.83 nm and 98.99 nm.

**Table 3.** Composition of CIGS elements by EDX characterization

| Element | Atomic % CIGS with |                  | Rasio Ga/(Ga+In) |                  |
|---------|--------------------|------------------|------------------|------------------|
|         | Pure Se            | SeO <sub>2</sub> | Pure Se          | SeO <sub>2</sub> |
| Cu      | 16.86              | 6.37             |                  |                  |
| In      | 18.47              | 18.13            | 0.067            | 0.106            |
| Ga      | 1.33               | 2.14             |                  |                  |
| Se      | 0.67               | 14.36            |                  |                  |

Table 3 shows the composition of CIGS elements using EDX characterization. Based on the data in Table 3, the At% of selenium derived from selenium dioxide was higher than selenium derived from pure selenium. This is happening because selenium dioxide is more soluble when compared to pure selenium [18], so using selenium dioxide will facilitate the growing CIGS on ITO substrates. Therefore, At% is very influential on the performance of solar cells. To achieve solar cells with high efficiency, At% of selenium must be 30% to 50%. This percentage makes defects in the film minimal so that CIGS as an absorber layer can function more optimally [2][23]. At% of CIGS films with pure selenium as a source of selenium is 0.67% and with selenium dioxide is 14.67%, so using selenium dioxide as a source of selenium in CIGS solar cells is better than pure selenium.

**Table 4.** Bandgap CIGS with pure selenium and selenium dioxide

| No | Sample                     | Bandgap (eV) |
|----|----------------------------|--------------|
| 1  | CIGS with Pure Se          | 1.03         |
| 2  | CIGS with SeO <sub>2</sub> | 1.06         |

To obtain a good CIGS solar cell, the ratio of Ga/(Ga+In) is 0.1-0.3 because, at that ratio, the defects in the CIGS film are smaller [9]. In Table 3, the Ga/(Ga+In) ratio of pure selenium is 0.067 and SeO<sub>2</sub> is 0.106, so it can be seen that the defects in CIGS films using SeO<sub>2</sub> are smaller than those of pure selenium. If the defects in the film are reduced, CIGS can function more optimally as an absorber layer. The use of pure selenium as a source of selenium in CIGS, in a Ga/(Ga+In) ratio of 0.067; this result did not meet the Ga/(Ga+In) ratio of the CIGS film, while the use of selenium dioxide as a source of selenium met the range of the Ga/(Ga+In) ratio. The CIGS band gap is about 1.01 eV to 1.60 eV [1], [5]. Bandgap CIGS can be obtained from the ratio Ga/(Ga+In) or GGI through the following equation [24]:

$$E_g = 1 + 0.564 \times GGI + 0.116 \times GGI^2 \tag{2}$$

based on equation (2), the bandgap of CIGS with pure selenium is 1.03 eV and with selenium dioxide 1.06 eV, shown in Table 4. This shows an increase in the bandgap of CIGS films with selenium dioxide as the source of selenium. CIGS performance will be more optimal if the CIGS band gap is close to 1.60 eV because it minimizes recombination and increases the Voc value [25].

When light hits the sample, there will be light absorption in layers because there is ZnO as a window layer, ZnS as a buffer layer, and CIGS as an absorber layer in a wide wavelength range so that it can be converted into the sunlight energy. The ability to convert energy from photons into electric charge by CIGS solar cells was measured using a solar simulator with a power of 100 mW cm<sup>-2</sup> and a sample area of 0.5 cm. Figure 4 and Table 5 show the results of testing CIGS solar cells using a solar simulator.

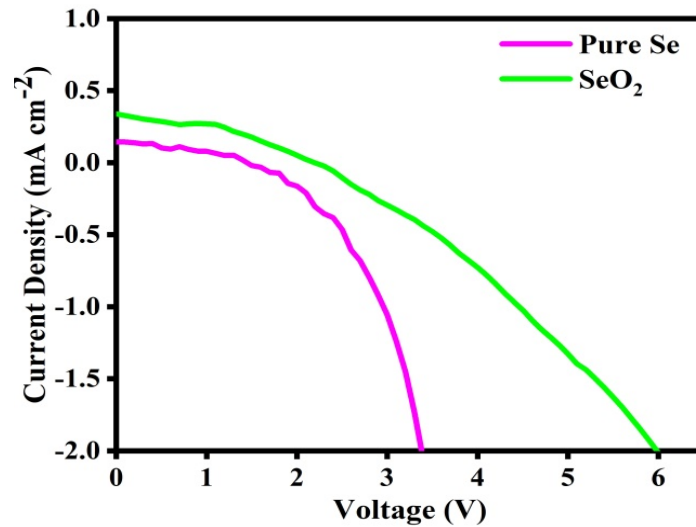


Figure 4. J-V characteristics of CIGS solar cells with the solar simulator

Table 5. Parameters of the J-V characteristics of CIGS solar cells with the solar simulator

| Sample           | Jsc (mA cm <sup>-2</sup> ) | Voc (V) | FF (%) | Efficiency (%) |
|------------------|----------------------------|---------|--------|----------------|
| Pure Se          | 0.143                      | 1.449   | 0.384  | 0.079          |
| SeO <sub>2</sub> | 0.376                      | 2.037   | 0.526  | 0.403          |

Based on the literature review described previously and the results of XRD analysis which shows the grain size of CIGS with SeO<sub>2</sub> is smaller than CIGS with Pure Se. If the grain size is small, the sample's surface area is more comprehensive so that the material's ability to store energy is more remarkable [24]. EDX analysts also showed that GGI CIGS with SeO<sub>2</sub> had smaller crystal defects than CIGS with Pure Se. The XRD and SEM-EDX analysis results relate to the data in Table 5; the value of Jsc, Voc, and FF solar cell CIGS with SeO<sub>2</sub> as a source of selenium is greater than that of pure selenium as a source of selenium. When the variable is significant, the efficiency as a benchmark for solar cell performance will also be more significant. The difference in efficiency is quite large, namely with pure selenium of 0.079% while with selenium dioxide (SeO<sub>2</sub>) of 0.4%. Thus, the use of selenium dioxide (SeO<sub>2</sub>) as a source of selenium will result in more excellent CIGS solar cell performance.

## Conclusions

In this study, selenium dioxide has synthesized and deposited using electrodeposition. Based on the results of XRF, SEM-EDX, and XRD data analysis, it can be concluded that the synthesis of selenium dioxide and deposition of CIGS by electrodeposition has been successfully carried out. Based on literature studies, comparisons with other studies, and characterization results, CIGS with selenium dioxide as a source of selenium will produce CIGS solar cells with high performance.

## Funding statement

The authors thank the Universitas Negeri Malang (UM) for the PNB (PUI-CAMRY) Research funding for NM group research.

## References

- [1] A. S. P. Dewi, N. Mufti, Arramel, B. H. Arrosyid, Sunaryono, and Aripriharta, "Synthesis and characterization of CIGS/ZnO film by spin coating method for solar cell application," AIP Conf. Proc., vol. 2231, no. April, 2020.

- [2] R.-W. You, K. K. Lew, and Y.-P. Fu, "Effect of indium concentration on electrochemical properties of electrode-electrolyte interface of  $\text{CuIn}_{1-x}\text{Ga}_x\text{Se}_2$  prepared by electrodeposition," *Mater. Res. Bull.*, vol. 96, pp. 183–187, 2017.
- [3] A. S. P. Dewi *et al.*, "Synthesis and characterization of CIGS ink by hot injection method," *AIP Conf. Proc.*, vol. 2228, no. April, 2020, doi: 10.1063/5.0000878.
- [4] K.-M. Huang, C.-L. Tsai, C.-Y. Chou, W.-J. Huang, and M.-C. Wu, "Electrodeposition of  $\text{CuIn}_{1-x}\text{Ga}_x\text{Se}_2$  Solar Cells on a Transparent Conducting Back Contact," in 2012 Asia-Pacific Power and Energy Engineering Conference, 2012, pp. 1–3.
- [5] N. Mufti *et al.*, "Review of CIGS-based solar cells manufacturing by structural engineering," *Sol. Energy*, vol. 207, no. July, pp. 1146–1157, 2020, doi: 10.1016/j.solener.2020.07.065.
- [6] H. X. Zhang and R. J. Hong, "CIGS absorbing layers prepared by RF magnetron sputtering from a single quaternary target," *Ceram. Int.*, vol. 42, no. 13, pp. 14543–14547, 2016.
- [7] C.-H. Huang, W.-J. Chuang, C.-P. Lin, Y.-L. Jan, and Y.-C. Shih, "Deposition technologies of high-efficiency CIGS solar cells: development of two-step and co-evaporation processes," *Crystals*, vol. 8, no. 7, p. 296, 2018.
- [8] M.-T. Sun, C.-T. Yang, Y.-C. Wu, and H.-I. Hsiang, "Effects of selenization process on densification and microstructure of  $\text{Cu}(\text{In}, \text{Ga})\text{Se}_2$  thin film prepared by doctor blading of CIGS nanoparticles," *Ceram. Int.*, vol. 44, no. 16, pp. 20508–20513, 2018.
- [9] C. Adel, B. M. Fethi, and B. Brahim, "Optical and electrical characterization of CIGS thin films grown by electrodeposition route," *Optik (Stuttg.)*, vol. 127, no. 8, pp. 4118–4122, 2016, doi: 10.1016/j.ijleo.2016.01.115.
- [10] C. Mahendran and N. Suriyanarayanan, "Effect of Bi incorporation and temperature on the properties of sprayed  $\text{CuInS}_2$  thin films," *Phys. B Condens. Matter*, vol. 408, pp. 62–67, 2013.
- [11] T. Tomai, Y. Nakayasu, M. Yanaka, and I. Honma, "Fabrication of  $\text{CuInSe}_2$  and  $\text{Cu}_2\text{ZnSnSe}_4$  films from metal-oxide precursors and  $\text{SeO}_2$  using supercritical ethanol," *J. Supercrit. Fluids*, vol. 101, pp. 48–53, 2015.
- [12] L. Laut, "Oleh Fitri," vol. XXXIX, pp. 55–63, 2014.
- [13] A. S. Maltsev, E. V. Chuparina, G. V. Pashkova, J. V. Sokol'nikova, O. V. Zarubina, and A. N. Shuliumova, "Features of sample preparation techniques in the total-reflection X-ray fluorescence analysis of tea leaves," *Food Chem.*, vol. 343, no. July, p. 128502, 2021, doi: 10.1016/j.foodchem.2020.128502.
- [14] C. Ossig *et al.*, "Four-fold multi-modal x-ray microscopy measurements of a  $\text{Cu}(\text{In}, \text{Ga})\text{Se}_2$  solar cell," *Materials (Basel)*, vol. 14, no. 1, pp. 1–12, 2021, doi: 10.3390/ma14010228.
- [15] P. M. S. Carvalho *et al.*, "Elemental mapping of Portuguese ceramic pieces with a full-field XRF scanner based on a 2D-THCOBRA detector," *Eur. Phys. J. Plus*, vol. 136, no. 4, pp. 1–16, 2021.
- [16] D. Tanini, C. Dalia, and A. Capperucci, "The polyhedral nature of selenium-catalysed reactions: Se (IV) instead of Se (VI) species make the difference in the mechanism of the on water selenium-mediated oxidation of arylamines," *Green Chem.*, 2021.
- [17] J. Kandasamy, S. Baranwal, and S. Gupta, "Selenium Dioxide Promoted  $\alpha$ -Keto N-Acylation of Sulfoximines Under Mild Reaction Conditions," *Asian J. Org. Chem.*
- [18] C. H. Review, "Selenium-catalyzed Functionalization of Alkynes," vol. 50, 2021, doi: 10.1246/cl.210065.
- [19] M. A. K. Mankoshi, F. I. Mustafa, and N. J. Hintaw, "Effects of Annealing Temperature on Structural and Optical Properties of CIGS Thin Films for Using in Solar Cell Applications," *J. Phys. Conf. Ser.*, vol. 1032, no. 1, 2018, doi: 10.1088/1742-6596/1032/1/012019.
- [20] B. Lara-Lara and A. M. Fernández, "CIGS thin film growing by electrodeposition technique using mechanical perturbation at the working electrode," *J. Mater. Sci. Mater. Electron.*, vol. 27, no. 5, pp. 5099–5106, 2016, doi: 10.1007/s10854-016-4400-1.
- [21] F. Long, W. Wang, J. Du, and Z. Zou, "CIS(CIGS) thin films prepared for solar cells by one-step electrodeposition in alcohol solution," *J. Phys. Conf. Ser.*, vol. 152, 2009, doi: 10.1088/1742-6596/152/1/012074.
- [22] A. Shongalova *et al.*, "Comparison of antimony selenide thin films obtained by electrochemical deposition and selenization of a metal precursor," *Mater. Today Proc.*, vol. 25, pp. 77–82, 2019, doi: 10.1016/j.matpr.2019.11.291.
- [23] H. Saïdi, C. Ben Alaya, M. F. Boujmil, B. Durand, J. L. Lazzari, and M. Bouaïcha, "Physical properties of electrodeposited CIGS films on crystalline silicon: Application for photovoltaic hetero-junction," *Curr. Appl. Phys.*, vol. 20, no. 1, pp. 29–36, 2020, doi: 10.1016/j.cap.2019.09.015.
- [24] J. Bäcker, "In situ investigation of the rapid thermal reaction of  $\text{Cu-In-Ga}$  precursors to  $\text{Cu}(\text{In}, \text{Ga})\text{Se}_2$  thin-film solar cell absorbers Jan-Peter Bäcker."
- [25] H. Sim, J. Lee, S. Cho, E. S. Cho, and S. J. Kwon, "A study on the band structure of  $\text{ZnO}/\text{CdS}$  heterojunction for CIGS solar-cell application," *J. Semicond. Technol. Sci.*, vol. 15, no. 2, pp. 267–275, 2015, doi: 10.5573/JSTS.2015.15.2.267.